Vol 17 No 4, April 2008
1674-1056/2008/17(04)/1480-10

Chinese Physics B

© 2008 Chin. Phys. Soc.
and IOP Publishing Ltd

A steered molecular dynamics study on the elastic behaviour of knotted polymer chains*

Shen Yu(沈 瑜)[a] and Zhang Lin-Xi(章林溪)[b]†

[a] *Department of Physics, Zhejiang University, Hangzhou* 310027, *China*

[b] *Department of Physics, Wenzhou University, Wenzhou* 325027, *China*

(Received 11 July 2007; revised manuscript received 21 November 2007)

In this paper the influence of a knot on the structure of a polymethylene (PM) strand in the tensile process is investigated by using the steered molecular dynamics (SMD) method. The gradual increasing of end-to-end distance, R, results in a tighter knot and a more stretched contour. That the break in a knotted rope almost invariably occurs at a point just outside the 'entrance' to the knot, which has been shown in a good many experiments, is further theoretically verified in this paper through the calculation of some structural and thermodynamic parameters. Moreover, it is found that the analyses on bond length, torsion angle and strain energy can facilitate to the study of the localization and the size of a knot in the tensile process. The symmetries of torsion angles, bond lengths and bond angles in the knot result in the whole symmetry of the knot in microstructure, thereby adapting itself to the strain applied. Additionally, the statistical property of the force-dependent average knot size illuminates in detail the change in size of a knot with force f, and therefore the minimum size of the knot in the restriction of the potentials considered in this work for a PM chain is deduced. At the same time, the difference in response to uniaxial strain, between a knotted PM strand and an unknotted one is also investigated. The force-extension profile is easily obtained from the simulation. As expected, for a given f, the knotted chain has an R significantly smaller than that of an unknotted polymer. However, the scaled difference becomes less pronounced for larger values of N, and the results for longer chains approach those of the unknotted chains.

Keywords: steered molecular dynamics, knotted polymer chain, united atom (UA) model
PACC: 8120S, 8200

1. Introduction

Entanglements are unavoidable in long polymers and influence their properties.[1−3] Knot theory[4−6] applied to the topology of macromolecules[1−3,7] indicates that the simple trefoil or 'overhand' knot has a high probability with which it exists in any long polymer strand,[8−11] and may exert an influence on the process of machining. Knots are also found in proteins,[12−18] and present an obstacle that needs overcoming in the transcription of DNA.[19] Fragments of DNA have been observed to contain such knots in experiment[20,21] and computer simulation.[22−26] An increasing number of experiments can now probe the detailed properties of knotted molecules.[21,27] Micromanipulation techniques[28−30] enable the direct measuring of mechanical properties of a single molecule, and it is even possible to probe the behaviour of artificially knotted DNA.[31] However, much remains unknown about the structures and properties of knots at the atomic level. For example, the minimum number of carbon atoms that can be sustained as a trefoil in a polyethylene strand is not well established.[7,8] Mathematically there are no knots in an open string, for continuous deformations can always bring it into an unentangled shape. However, appropriate stretching may enable the knot to exist and simultaneously make it tighter and tighter, which enables us to study the structural and the mechanical properties and the dynamical behaviours of knotted polymer chains in detail.

Polymethylene or polyethylene is the simplest polymer and therefore an excellent generic system for realizing various experimental and theoretical intentions.[32,33] In this work, we apply the knot to a strand with unlinked ends, as done in Ref.[34], and ob-

*Project supported by the National Natural Science Foundation of China (Grant Nos 20274040, 20574052 and 20774066), the Program for New Century Excellent Talents in University, China (Grant No NCET-05-0538) and the Natural Science Foundation of Zhejiang Province, China (Grant No R404047).

†Corresponding author. E-mail: Lxzhang@hzcnc.com

tain the force extension profiles, structure properties and localization while the polymethylene (PM) strand is stretching. An important advantage of using the SMD method is that the force can be directly obtained in the stretch process. Compared with the molecular dynamics (MD) method, the steered molecular dynamics (SMD) means the expediting of conformational changes in macromolecular systems through the action of time-dependent external forces. Using this technique, one can investigate the molecular mechanisms that determine elastic properties exhibited by macromolecules subjected to deformations in atomic force microscopy (AFM) and optical tweezer experiments, overcome slow natural time scales and explore putative conformational pathways. In the process, the force acts on the terminal monomers via a spring. Intrachain differentiations in bond lengths, torsion angles and bond angles are calculated to obtain the localization of the knot, while changes of these parameters in the process of extension are given to characterize the changes of the knot in size and shape. Combination information about bond lengths, torsion angles and bond angles can provide some insights into the microstructure as well. Energy distribution is studied to show the stress distribution from exogenic action. Additionally, statistical properties such as the average knot size as a function of force is plotted to present the change in number of bonds within the knot and facilitate to the approximate deduction of the critical size of the knot in a chain when force action is large enough. At the same time, we can also obtain the difference in response to uniaxial strain, between a knotted PM strand and an unknotted one.

2. Model and method

2.1. Potentials

In this study we perform molecular dynamics simulations for polymethylene (PM) chains with the values of chain length N being 79, 99 and 119 (namely, with 80, 100 and 120 carbon atoms) by using the united atom (UA) model.[35] In the UA model, methyl or methylene groups are replaced by single interaction sites located at the carbon atoms, with hydrogen atoms neglected. The UA model reflects the effects of hydrogen atoms on the potential parameters and can reduce computational cost significantly. The force fields for polymethylene chains have been previously employed in bulk phase simulation,[36−38] and gave reliable thermodynamic and structural properties as well as dynamic properties such as self-diffusivity and local chain motions in agreement with ^{13}C NMR spin-lattice (T_1) relaxation.[36] Using such a force field, we investigate structural and mechanical responses of a knotted PM chain and an unknotted one to the uniaxial extension.

The UA force field for n-alkanes used in the present simulation is listed as follows:

Here, instead of the rigid bond length, a stiff harmonic spring is assumed to be between any two connected beads. The harmonic potential is expressed as

$$V_{\text{bond}} = \sum_{i=2}^{N} k_b(|\boldsymbol{u}_i| - \sigma)^2/2. \tag{1}$$

Without being constricted or stretched, the monomers are naturally connected to the adjacent one by a virtual bond of length $\sigma = 0.153\,\text{nm}$, which is the average distance between consecutive C atoms in polymethylenes. $\boldsymbol{u}_i = \boldsymbol{r}_i - \boldsymbol{r}_{i-1}$ is the bond vector and $\boldsymbol{r}_i$ is the location of bead i. The spring constant is k_b=6.34×10^4 kcal/(mol·nm^2).

The nonbonded potential between sequence-distant beads is represented as a sum of pairwise potentials:

$$V_{\text{nonbonded}} = \sum_{|i-j|\geq 4} \varepsilon\left[\left(\frac{\Delta r_m}{\boldsymbol{r}_j - \boldsymbol{r}_i}\right)^{12} - 2\left(\frac{\Delta r_m}{|r_j - r_i|}\right)^{6}\right], \quad r < 0.9\,\text{nm}, \tag{2}$$

where Δr_m is set to be 0.45 nm. The value of ε depends on the types of monomers i and j. For $CH_2\cdots CH_2$, $CH_3\cdots CH_3$, and $CH_2\cdots CH_3$, the values of ε are 0.09344, 0.22644 and 0.14546 kcal/mol, respectively.

The bond angle among three successive beads is constrained by a harmonic potential. Therefore, the bending potential is written as

$$V_{\text{bend}} = \sum_{i=2}^{N-1} k_\theta(\cos\theta_i - \cos\theta_0)^2/2, \tag{3}$$

where θ_0=1.920 rad is the equilibrium bending angle, θ_i is the angle between vectors $\boldsymbol{u}_i$ and $\boldsymbol{u}_{i+1}$, and k_θ=120 kcal/mol.

The dihedral angle potential (torsion angle potential), involving four successive beads, is represented by

$$V_{\text{dih}} = \sum_{i=2}^{N-2} \frac{1}{2}\{k_\varphi^1(1-\cos\varphi_i) + k_\varphi^2(1-\cos2\varphi_i) + k_\varphi^3(1-\cos3\varphi_i)\}, \tag{4}$$

where k_φ^1=1.6 kal/mol, k_φ^2=–0.867 kal/mol and k_φ^3=3.24 kal/mol. The dihedral angle φ_i is formed between the vectors $\boldsymbol{d}_i = \boldsymbol{u}_i \times \boldsymbol{u}_{i+1}$ and $\boldsymbol{d}_{i+1} = \boldsymbol{u}_{i+1} \times \boldsymbol{u}_{i+2}$.

Specifically, the potential energy of a given conformation of a polymethylene strand is given by

$$V = V_{\text{bond}} + V_{\text{nonbonded}} + V_{\text{bend}} + V_{\text{dih}}. \quad (5)$$

2.2. Simulation of the dynamics

For each of the 3 (N+1) degrees of freedom of the model polymer (x, y or z coordinates of the carbon atoms), the Langevin equation[39–42] of motion is

$$m\dot{v}(t) = F_{\text{conf}} - m\gamma v(t) + \eta(t), \quad (6)$$

where m, v, $\dot{v}$, F_{conf}, γ and η are, respectively, mass, speed, acceleration, conformational force, friction (viscosity) constant and random force having a white noise spectrum. The conformational force is equal to the negative gradient of the total potential energy for a given model, and η is drawn from a Gaussian distribution, of which the variance is determined by the temperature of the system (see Eq.(3) in Ref.[43]). Each carbon atom is subjected to a random force at each integration time step. The components of the random force are independently generated by setting $\eta_i = (2m\gamma k_{\text{B}}T/\delta t)^{1/2}\xi_i$, where i denotes the uncorrelated random force components in the x, y and z directions, ξ_i is a random value taken from a Gaussian distribution with zero mean and unit variance (obtained from a random number generator by standard techniques);[44] δt is the integration time step. Additionally, In order to keep the temperature constant, the speeds of all monomers are scaled by a factor

$$\lambda = \left(1 + \frac{\Delta t}{t_T}\left(\frac{T}{T_{\text{c}}} - 1\right)\right)^{\frac{1}{2}} \quad (7)$$

where T_{c} is the current kinetic temperature, T denotes the desired temperature, and t_T is a preset time constant. Berendsen *et al* [45] have found that a suitable relaxation time is t_T=0.4 ps. In this work, the system temperature is fixed at T=280 K. And then the random force η is set to be 0 for simplicity in our simulation.

To study the elastic behaviour of knotted polymer chains, an extra force via a spring is added to bead N+1 to extend the chain (see Fig.1). Illustrated are two conformations of a knotted chain, with one of its ends fixed and the other one (bead N+1) attached to a linear spring (force probe). The end-to-end distance,R, increases along the tensile direction in the process of pulling, thereby showing a force-extension profile. The stiffness of the spring is k_0=945 pN/nm, and it moves at a constant speed v=5×10^{-3} nm/ps. The force probed by the spring is therefore given by Hook's law,$f = k_0(z_0 - z_1)$, where z_1 and z_0 are the displacements of the last monomer and the spring's opposite end point respectively. Thus, for bead N+1, components of f in the x, y and z directions should respectively be added to the right-hand side of Eq.(6). In this work, pulling speed v=5×10^{-3} nm/ps is not large, and then the influence of the friction is relatively small, so here γ is set to be 0 for simplicity. We have also made a comparison between the results of bond length distribution with γ=0 and γ=0.01 as an example, and find that the difference is rather trivial. $v = 10^{-3} - 0.05$ nm/ps has been adopted in other works (see Ref.[46]).

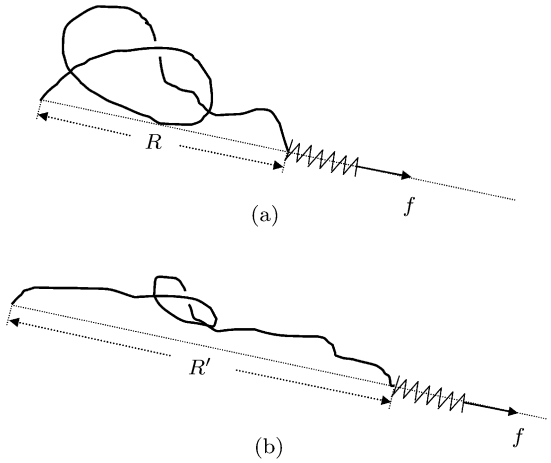


Fig.1. Two conformations of a knotted chain, with one of its ends fixed and the other one attached to a linear spring (force probe). The end-to-end distance increases along tensile direction in the process of stretching.

If the time step is Δt, the position and the velocity of bead i at the time $t + \Delta t$ are respectively expressed by Beeman[47] as

$$\boldsymbol{r}_i(t + \Delta t) = \boldsymbol{r}_i(t) + \boldsymbol{v}_i(t)\Delta t + \frac{4\boldsymbol{F}_i(t) - \boldsymbol{F}_i(t - \Delta t)}{6m}\Delta t^2 \quad (8)$$

and

$$\boldsymbol{v}_i(t + \Delta t) = \boldsymbol{v}_i(t) + \frac{2\boldsymbol{F}_i(t + \Delta t) + 5\boldsymbol{F}_i(t) - \boldsymbol{F}_i(t - \Delta t)}{6m}\Delta t, \quad (9)$$

where $\boldsymbol{v}_i$ denotes the velocity of bead i and Δt is set to be 0.001ps in this paper. $\boldsymbol{F}_i$ is the resultant force on bead i: $\boldsymbol{F}_i = m\dot{\boldsymbol{v}}_i$ is a vectorial form of Eq.(6).

Therefore, using the simulation method above, the force-extension curves of the system can be easily obtained by pulling the chain apart at a constant speed. Moreover, the evolvement of a knot in the pulling process and the influence on microstructure and energy distribution of the chain can also be investigated.

One can assume from the outset in the analysis of simulation results that systems described are not in equilibrium and then one may employ the nonequilibrium description of the analysis. That is possible in principle, which has been shown in the work of Jarzynski,[48,49] who demonstrated that free energy differences could be obtained through exponential averages of irreversible work.

3. Results and discussion

We have performed several tests for the elastic behaviours of a knotted PM chain and an unknotted PM chain. One of their results is presented in this paper; the rest are similar, and they are different only by the localization of the knot. Four representative conformations of a knotted chain in the stretch process are plotted in Fig.2, and Figs.2(a), 2(b), 2(c) and 2(d) denote the conformations at t=600, 2100, 4200 and 6300 ps, respectively. Timing starts with a force acting on the chain via a linear spring, and then gradually increasing end-to-end distance, R, results in a tighter knot and a more stretched contour. It can also be seen from these figures that while pulling on a string makes a knot tight, the knot begins to localize tightly at a small portion of the chain. However, in a random unforced chain the knot is spread over the whole curve. The knot sizes and two entrance bonds at different values of time t are marked in the plots. Knot size is measured by counting the number of the bonds within the knot. Accordingly, in the process of pulling, microstructure such as bond length, torsion angle and bond angle distributions will change as well, which is discussed below in detail.

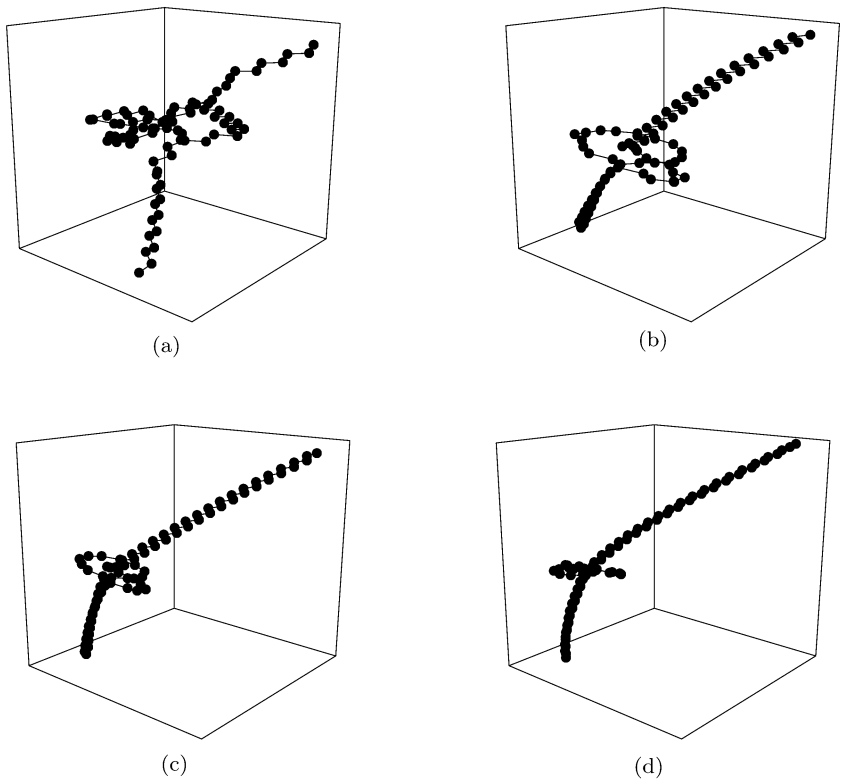


Fig.2. Four representative conformations of a knotted PM chain in the process of evolution when the chain is stretched. Panel (a) denotes a conformation at t=600 ps, with knot spread over the curve; Panel (b) denotes a conformation at t=2100 ps, with a knot size N_k=28, from bonds 22 to 49; Panel (c) denotes a conformation at t=4200 ps, with a knot size N_k=21, from bonds 24 to 44; Panel (d) denotes a conformation at t=6300 ps, with a knot size N_k=19, from bonds 24 to 42. The pulling speed is 5×10^{-3} nm/ps and the temperature is T=280K. Gradually increasing end-to-end distance R results in a tighter knot and a more stretched contour.

Figure 3 shows the evolution of the bond length distribution during the structural tension of a 79-bond knotted polymethylene (PM) chain (a) and an unknotted one before breaking occurs (b), and i is the serial number of bonds. Here, the criterion of numbering, based on that in Ref.[50], is that the carbon atoms, the carbon bonds, the bond angles and the torsion angles in a chain with chain length $N = 79$ are respectively marked from 0 to 79, from 1 to 79, from 1 to 78 and from 3 to 79. In the bond length distribution curves for the knotted chain, two peaks separately occur at $i = 22$ and $i = 49$ when t=2100 ps, at $i = 24$ and $i = 44$ when t=4200 ps, and at $i = 24$ and $i = 42$ when t=6300 ps. Comparing the results with the corresponding structures shown in Fig.2, we find that two peaks in the bond length distribution curve always separately correspond to the two symmetric bonds that are just at the entrance to the knot. The localization and the size of the knot can then be obtained intuitionally in the plots. The diminution of the separation between two peaks suggests that the number of carbon bonds which sustain the knot decreases gradually in the tensile process, indicating that with the extension of the chain, the knot becomes tighter and tighter. Under stress, the middle bond of the knot is protected in some degree by the side ones, so the middle bond length is observably smaller. Importantly, we may alternatively identify knotted segments in this manner. In Fig.3(b), we find that for an unknotted chain, the bond length changes little with i, and it is the fact that the transmission of strain from the end-of-chain (acting with a linear spring) to the beginning-of-chain cannot keep up with the tensile speed v results in the phenomenon in which the bond with a large code number i is slightly longer than that with a small one.

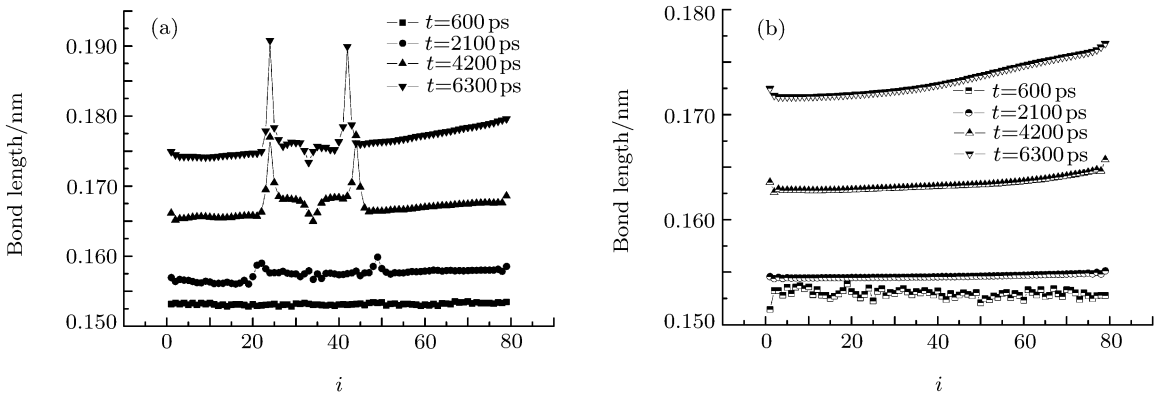


Fig.3. Bond length distributions in the tensile process. Shown is the distribution along a knotted polymethylene (PM) chain (a) and an unknotted one (b) with a chain length $N = 79$. For the knotted chain, two peaks in the bond length distribution curve separately occur at $i = 22$ and 49 when t=2100 ps, at $i = 24$ and 44 when t=4200 ps, and at $i = 24$ and 42 when t=6300 ps. Here i is the serial number of bonds in the PM chain, and marked from 1 to 79 for a 79-bond PM chain.

The bond angle distributions along a knotted PM chain and an unknotted PM chain in the tensile process with a chain length $N = 79$ are given in Fig.4, and Figs.4(a), 4(b) and 4(c) denote the conformations at t=2100, 4200 and 6300 ps, respectively. In these figures, i is the serial number of bond angles in the chain, and marked from 1 to 78 for a 79-bond chain. From the plots, we find that there exists an exceptional region with two peaks in the curves of bond angle distribution for a knotted chain, and the two peaks occur at i=21 and 49 when t=2100 ps, at i=23 and 44 when t=4200 ps, and at i=22 and 43 when t=6300 ps, separately. Using the criterion of numbering, we see that at t=2100 and 4200 ps, two peaks occur at the bond angles that are just outside the entrance to the knot, and the number of bond angles between two peaks is the same as those in Figs.2 and 3; while at t=6300 ps, there exist more bond angles between the two "peak" bond angles than that in Figs.2 and 3, which may indicate that when the chain is strongly stretched, the tightest knot will disturb its neighbouring bond angles as well. When the chain is stretched to some degree,

the average value of bond angles within the knot becomes unchanged, and the mean value is 2.45 at t=4200 and 6300 ps. We assume that the mean value of 2.45 is of a balanced state for the elongation of the whole chain and the tightness of the knot. However, the bond angles outside the knot maintain right angles with t increasing, indicating that the chain becomes more stretched on the whole in the tensile process. From the plots we also notice a phenomenon in which the middle point of the knot always tends to keep consistent with the bond angles outside the knot and bond angles in two sides of the middle point are symmetrical, which can help us understand the microstructure of the knot in a stretched chain. Aside from the prominent abnormity of the bond angles in the knot, the bond angles at the ends of the chain are also exceptional due to the fixation of the first monomer and the pulling of the last monomer. At the same time t in the tensile process, the bond angle of the unknotted chain is smaller than that of the knotted one because of the difference in structure.

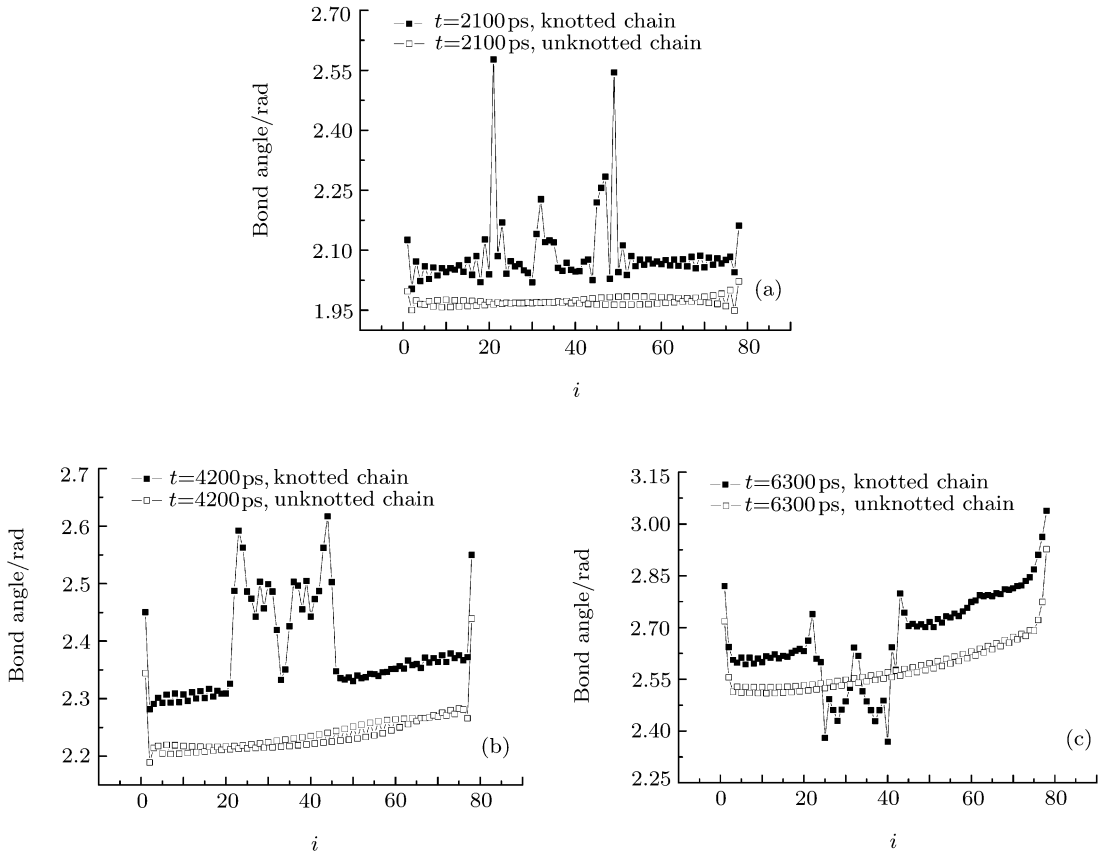


Fig.4. Bond angle distributions in the tensile process. Shown is the distribution along a knotted PM chain and an unknotted PM chain with a chain length $N = 79$. Panel (a) denotes conformations at t=2100 ps; Panel (b) denotes conformations at t=4200 ps; Panel (c) denotes conformations at t=6300 ps. For the knotted chain, two peaks in the bond angle distribution separately occur at $i = 21$ and 49 when t=2100 ps, at $i = 23$ and 44 when t=4200 ps, and at $i = 22$ and 43 when t=6300 ps. Here i is the serial number of bond angles in the PM chain, and marked from 1 to 78 for a 79-bond PM chain.

Accordingly, it is natural to identify a segment where the knot is located, and consequently to talk about its size and statistics from the analysis to the torsion angle distribution in the tensile process as well, which can be seen in Fig.5. Figures 5(a), 5(b) and 5(c) separately denote conformations of knotted and unknotted PM chains at different values of time t in the course of pulling. Here, i is the serial number of torsion angles in the chain, and it is marked from 3 to 79 for a 79-bond chain. For an unknotted chain, all torsion angles are equal to about 3.14, suggesting the coplanarity of the bonds and monomers, a conse-

quence of extension. However, for a knotted chain, the knot cannot be coplanar because of the excluded volume effect and intrachain potential restriction. Thus the values of torsion angles involved in the knot deviate from 3.14, forming an exceptional region in the torsion angle distribution curve. In the curves for the knotted chain, at t=2100 ps, the region starts at $i = 22$ and ends at $i = 51$; at t=4200 ps, the region starts at $i = 24$ and ends at $i = 46$; and at t=6300 ps, the region starts at $i = 24$ and ends at $i = 44$. Using the criterion of numbering, we find that this result is exactly consistent with the case in Figs.2 and 3. The evolution of the range that denotes the dwelling of the knot implies that the knot becomes tighter and tighter in the tensile process, which is consistent with the results of the bond length distribution. Through studying the values of torsion angles we can determine the localization and the size of the knot in the chain as well. Obviously, the middle turn in the torsion angles within the knot ensures the success of knotting. Additionally, the symmetry of the torsion angles in the knot, together with the symmetries in bond length and bond angle discussed above, results in further symmetry of the knot in microstructure, and thereby adapting itself to the strain applied. Combination of bond length, bond angle and torsion angle can provide detailed information about the microscopic conformations in the tensile process.

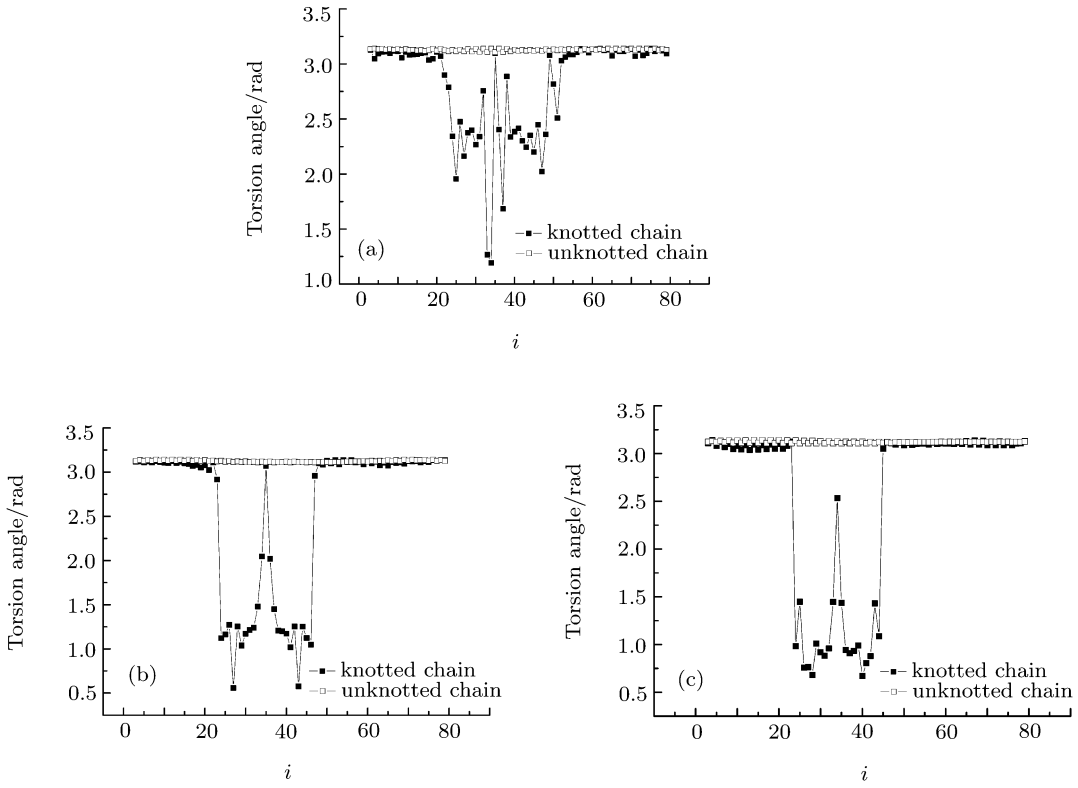


Fig.5. Torsion angle distribution in the tensile process. Shown is the distribution along a knotted PM chain and an unknotted PM chain with N=79. Panel (a) denotes conformations at t=2100 ps; panel (b) denotes conformations at t=4200 ps; panel (c) denotes conformations at t=6300 ps. For the knotted chain, at t=2100 ps, the region in which the value of torsion angles deviates from about 3.14, starts at $i = 22$ and ends at $i = 51$; at t=4200 ps, the region starts at $i = 24$ and ends at $i = 46$; at t=6300 ps, the region starts at $i = 24$ and ends at $i = 44$. Here i is the serial number of torsion angles in the chain, and marked from 3 to 79 for a 79-bond PM chain.

Tensions of the strain energy distribution along a knotted 79-bond PM chain (a) and an unknotted one (b) are shown in Fig.6. Here i is the serial number of bonds in the chain. The strain energy localizes mostly on bond 22 and bond 49 when t=2100 ps, on bond 24 and bond 44 when t=4200 ps, and on bond 24 and bond 44 when t=6300 ps. These bonds are just at the entrance to the knot, which is consistent with the cases in Figs.2–4. In other words, while the knotted chain is pulling, the stress tends to concentrate mostly

on the two entrance bonds, which indicates that the knot weakens the strand significantly, and that, like a knotted rope, it breaks under tension at the entrances to the knot. In the same way, the energy of the middle bond within the knot is remarkably smaller than those of the side ones. Similarly, that the transmission of energy from the end-of-chain (acting with linear spring) to the beginning-of-chain cannot keep up with the tensile speed v results in the phenomenon in Fig.6(b), in which for an unknotted chain, energy of bond increases slightly with serial number i under tension.

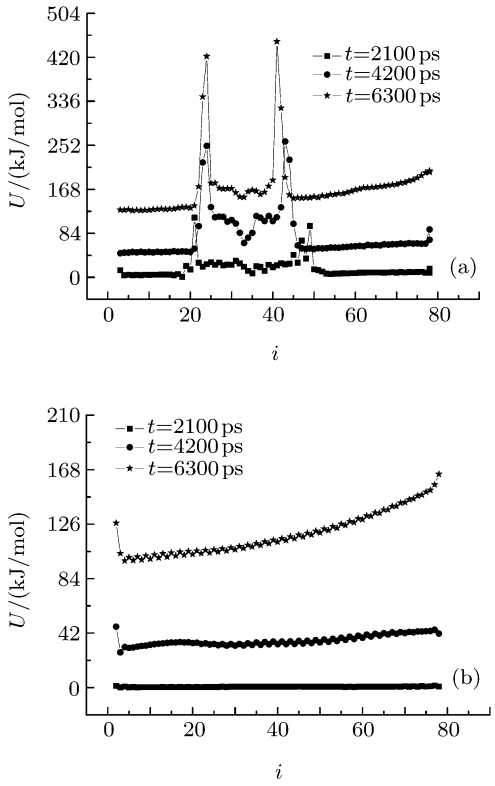


Fig.6. Strain energy distributions in the tensile process. Shown is the distribution along a knotted PM chain (a) and an unknotted PM chain (b) with a chain length N=79. For the knotted chain, two peaks in the strain energy distribution curve separately occur at i = 22 and 49 when t=2100 ps; at i = 24 and 44 when t=4200 ps; at i = 24 and 42 when t=6300 ps. Here i is the serial number of bonds in the PM chain, and marked from 1 to 79 for a 79-bond chain.

Figure 7 depicts the results of force-extension relationships for knotted and unknotted chains with different values of chain length N. f is the external force obtained via Hook's law for a spring, and R is the mean end-to-end distance of a chain. In the process of tensile elongation, the values of elastic force f for knotted and unknotted chains both increase with R. For unknotted chains, f increases linearly with R due to its linear contour, while f for knotted chains increases nonlinearly due to the influence of the knot. As expected, for a given f the knotted polymer has an R significantly smaller than an unknotted polymer. However, the scaled difference becomes less pronounced for larger values of N, and the results for longer chains approach those of the unknotted chains.

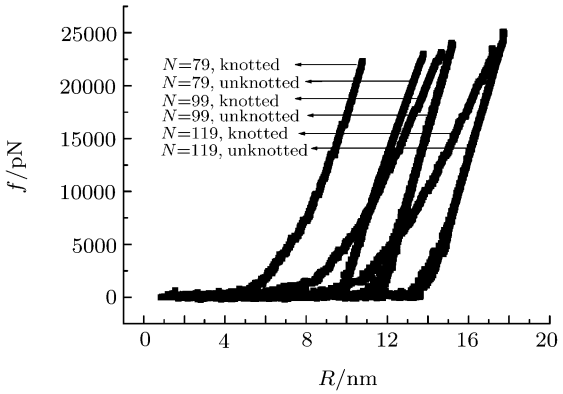


Fig.7. The curves for scaled force f as a function of the end-to-end distance R, for knotted and unknotted chains with the values of chain length N being 79, 99 and 119, respectively.

In the simulation, the mean knot size $< N_k >$ as a function of force f for chains with N=79, 99 and 119 is also investigated, and the results are plotted in Fig.8. $< N_k >$ is the average number of carbon bonds within the knot. We see that the plots of $< N_k >$ as a function of f can be fitted with a linear equation $< N_k >= A + B/f$ as shown in the plot. For N =79, 99 and 119, A equals 15.99, 16.37 and 16.38 respectively, showing that A is independent of chain

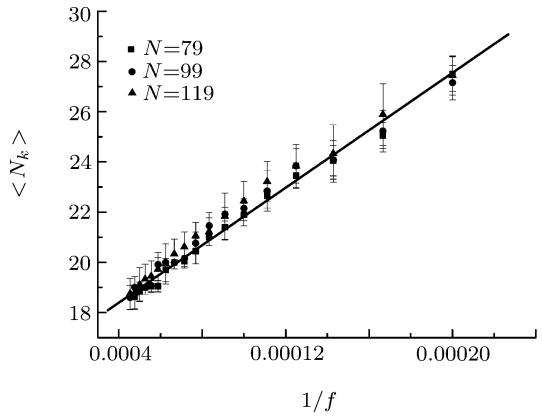


Fig.8. The curves for average size of knots $< N_k >$ as a function of the force f for PM chains with N= 79, 99 and 119, respectively. Here $< N_k >$ is the number of bonds within the knot, averaged over 40 samples.

length N within an allowance error. From the fitting equation, we know that A denotes the number of carbon bonds involved in the knot when f applied approaches infinity, thereby we can obtain the information that the minimum number of bonds to sustain a knot will not be less than about 16 because of the primary restriction of intrachain potentials and regardless of chain length.

4. Summary

We have investigated the elastic behaviours of a knotted polymethylene (PM) strand and how the knot in the chain behaves in the tensile process. Using the SMD method, the force-extension profile is easily obtained. Gradually increasing end-to-end distance R results in a tighter knot and a more stretched contour. As expected, for a given f, the knotted polymer has an R significantly smaller than an unknotted polymer. However, the scaled difference becomes less pronounced for larger values of N, and the results for longer chains approach those of the unknotted chains. The symmetries of torsion angles, bond lengths and bond angles result in the whole symmetry of the knot in microstructure, and thereby adapting itself to the strain applied. Combination information of bond length, bond angle and torsion angle can provide the detailed information about microscopic conformations in the tensile process. The strain energy distribution shows that while the knotted chain is pulling, the stress tends to concentrate mostly on the two entrance bonds, which indicates that the knot weakens the strand significantly, and that, like a knotted rope, it breaks under tension at the entrances to the knot. Additionally, statistical property $< N_k > \sim 1/f$ illuminates in detail the change in size of a knot with a force, f, applied, and therefore the minimum knot size in the restriction of the potentials considered is deduced in this work. Our present methods and results have shown much important information for a knotted chain to be pulled apart and can also provide a good approach to the study of more complicated systems with topological entanglement.

References

[1] Mislow K 1965 *Introduction to Stereochemistry* (New York: Benjamin) p110

[2] Schill G 1971 *Catenanes, Rotaxanes, and Knots* (New York: Academic) p43

[3] Walba D M 1985 *Tetrahedron* **41** 3161

[4] Atiyha M F 1990 *The Geometry and Physics of Knots* (Cambridge University Press) p291

[5] Katritch V, Bednar J, Michoud D, Scharein R G, Dubochet J and Stasiak A 1996 *Nature* **384** 142

[6] Katritch V 1997 *Nature* **388** 148

[7] Frisch H L and Wasserman E 1961 *J. Am. Chem. Soc.* **83** 3789

[8] Frank-Kamenetskii M D, Lukashin A V and Vologodskii A V 1975 *Nature* **258** 398

[9] Frisch H L 1993 *New J. Chem.* **17** 679

[10] Mansfield M L 1994 *Macromolecules* **27** 5924

[11] van Rensburg E J, Sumners D A W, Wasserman E and Whittington S G 1992 *J. Phys.* A **25** 6557

[12] Taylor W R 2000 *Nature* **406** 916

[13] Michel G, Sauve V, Larocque R, Li Y, Matte A and Cygler M 2002 *Structure* **10** 1303

[14] Nureki O, Watanabe K, Fukai S, Ishii R, Endo Y, Hori H and Yokoyama S 2004 *Sturcture* **12** 593

[15] Zarembinski T I, Kim Y, Peterson K, Christendat D, Dharamsi A, Arrowsmith C H, Edwards A M and Joachimiak A 2003 *Proteins: Struct. Funct. Genet.* **50** 177

[16] Taylor W R and Lin K 2003 *Nature* **406** 916

[17] Mallam A L and Jackson S E 2006 *J. Mol. Biol.* **359** 1420

[18] Mallam A L and Jackson S E 2005 *J. Mol. Biol.* **346** 1409

[19] Alberts B, Robert K, Bray D, Lewis J, Raff M and Watson J D 1994 *The Molecular Biology of the Cell* (New York: Garland) p38

[20] Wasserman S A and Cozzarelli N R 1986 Science **232** 951

[21] Shaw S Y and Wang J C 1993 *Science* **260** 533

[22] Moore T N, Rhonald C L and Grosberg Y A 2004 *Proc. Natl. Acad. Sci. USA* **101** 13431

[23] Virmau P, Kantor Y and Kardar M 2005 *J. Am. Chem. Soc.* **127** 15102

[24] Pik-Yin L 2002 *Phys. Rev.* E **66** 021805

[25] Liu Z R, Jennifer K M, Lynn Z E and Chan H S 2006 *J. Mol. Biol.* **361** 268

[26] Farago O, Kantor Y and Karadar M 2002 *Europhys. Lett.* **60** 53

[27] Rybenkov V V, Cozzarelli N R and Vologodskii A V 1993 *Proc. Natl. Acad. Sci. USA* **90** 5307

[28] Smith S B, Finzi L and Bustamante C 1992 *Science* **258** 1122

[29] Smith S B, Cui Y and Bustamante C 1996 *Science* **271** 795

[30] Ashkin A 1997 *Proc. Natl. Acad. Sci. USA* **94** 4853

[31] Arai Y, Yasuda R, Akashi K I, Harada Y, Miyata H, Kinosita K jr and Iton H 1999 *Nature* **399** 446

[32] Zhang F Q, Yang J L, Li Z H, Ying C T and Liu G J 2007 *Acta Phys. Sin.* **56** 3577 (in Chinese)

[33] Teng F E, Han W, Liu Y L and Wang Y M 1991 *Acta Phys. Sin.* **40** 1955 (in Chinese)

[34] Ashley C W 1993 *The Ashley Book of Knots* (New York: Doubleday) p67

[35] Chang J, Han J, Yang L, Jaffe R L and Yoon D Y 2001 *J. Chem. Phys.* **115** 2831

[36] Smith G D and Yoon D Y 1994 *J. Chem. Phys.* **100** 649

[37] Paul W, Yoon D Y and Smith G D 1995 *J. Chem. Phys.* **103** 1702

[38] Han J, Jaffe R L and Yoon D Y 1997 *Macromolecules* **30** 7245

[39] Wallin S and Chan H S 2006 *J. Phys.: Condens. Matter* **18** S307

[40] Chen Y, Huang Z G, Wang Y H and Zhang Y 2007 *Chin. Phys.* **16** 975

[41] Wu X Z, Yang H J and Zhuo Y Z 1994 *Chin. Phys.* **3** 539

[42] Dou S X, Wang P Y and Xie P 2004 *Chin. Phys.* **13** 1569

[43] Kaya H and Chan H S 2003 *J. Mol. Biol.* **326** 911
Kaya H and Chan H S 2003 *J. Mol. Biol.* **337** 1069 (corrigendum)

[44] Allen M P and Tildesley D J 1987 *Computer Simulation of Liquids* (Oxford: Oxford University Press) p71

[45] Berendsen H J, Postma J P M, van Gunsteren W F, DiNola A and Haak J R 1984 *J. Chem. Phys.* **81** 3684

[46] Marrink S J, Berger O, Tieleman P and Jähnig F 1998 *Biophys. J.* **74** 931

[47] Beeman D 1976 *J. Comp. Phys.* **20** 130

[48] Jarzynski C 1997 *Phys. Rev. Lett.* **78** 2690

[49] Jarzynski C 1997 *Phys. Rev.* E **56** 5018

[50] Flory P J 1969 *Statistical Mechanics of Chain Molecules* (New York: Interscience) p44